scientific reports

Check for updates

OPEN

Exercise induces dynamic changes in intra-articular metabolism and inflammation associated with remodeling of the infrapatellar fat pad in mice

Timothy M. Griffin[1,2,3]✉, Ravi K. Komaravolu[1], Erika Barboza Prado Lopes[1], Padmaja Mehta-D'souza[1], Taylor Conner[1], Tessa Kovats[1], Susan Kovats[4], Madeline Allen[5], Peyton Harris[6], Mary Beth Humphrey[2,7], Hope D. Welhaven[8], Priyanka Brahmachary[9] & Ronald K. June[9]

We hypothesized that daily exercise promotes joint health by upregulating anti-inflammatory mediators via adaptive molecular and metabolic changes in the infrapatellar fat pad (IFP). We tested this hypothesis by conducting time-resolved analyses between 1 and 14 days of voluntary wheel running exercise in C57BL/6J mice. IFP structure and cellularity were evaluated by histomorphology, picrosirius red collagen staining, and flow cytometry analysis of stromal vascular fraction cells. Joint inflammation and metabolism were evaluated by multiplex gene expression analysis of synovium-IFP tissue and synovial fluid metabolomics, respectively. Exercise transiently increased cytokine and chemokine gene expression in synovium-IFP tissue, resolving within the first 5 days of exercise. The acute inflammatory response was associated with decreased adipocyte size and elevated $CD45^+Gr1^+$ myeloid cells, increased collagen content, and oxidized phospholipids. Exercise acutely altered synovial fluid metabolites, characterized by increased amino acids, peptides, bile acids, sphingolipids, dicarboxylic acids, and straight medium chain fatty acids and decreased hydroxy fatty acids and diacylglycerols. Between 5 and 14 days of exercise, inflammation, collagen, and adipocyte size returned to pre-exercise levels, and $CD206^+$ immuno-regulatory macrophages increased. Thus, although the onset of new daily exercise transiently induced synovium-IFP inflammation and altered tissue structure, sustained daily exercise promoted IFP homeostasis.

Keywords Hoffa's fat pad, Adipocyte, Synovium, Metabolomics, Metaflammation, Running, Fibrosis, Knee

Abbreviations

ANOVA	Analysis of variance
β-AR	Beta-adrenergic receptor
CSA	Cross sectional area
DAMPs	Damage-associated molecular patterns
GM-CSF	Granulocyte-macrophage colony-stimulating factor

[1]Aging and Metabolism Research Program, Oklahoma Medical Research Foundation, 825 NE 13th St, Oklahoma City, OK 73104, USA. [2]Veterans Affairs Medical Center, Oklahoma City, OK 73104, USA. [3]Oklahoma Center for Geroscience, Department of Biochemistry and Molecular Biology, University of Oklahoma Health Sciences Center, Oklahoma City, OK 73104, USA. [4]Arthritis and Clinical Immunology Research Program, Oklahoma Medical Research Foundation, Oklahoma City, OK 73104, USA. [5]Department of Health and Exercise Science, University of Oklahoma, Norman, OK 73019, USA. [6]Department of Biology, University of Oklahoma, Norman, OK 73019, USA. [7]Department of Medicine, Department of Microbiology and Immunology, University of Oklahoma Health Sciences Center, Oklahoma City, OK 73104, USA. [8]Department of Chemistry & Biochemistry, Montana State University, Bozeman, MT 59717, USA. [9]Department of Mechanical & Industrial Engineering, Montana State University, Bozeman, MT 59717, USA. ✉email: Tim-Griffin@omrf.org

FAPs	Fibro-adipogenic progenitors
IFP	Infrapatellar fat pad
IL-10	Interleukin-10
MRI	Magnetic resonance imaging
OA	Osteoarthritis
PCA	Principal component analysis
SVF	Stromal vascular fraction
$TLR4^{-/-}$	Toll-like receptor 4 genetic mutant
TNF	Tumor necrosis factor
WT	Wild type

Synovial joints function as complex organs, being composed of various tissue types that differ in anatomical structure, biological regulation, and material properties. Understanding the integrated function of different joint tissues and cells provides insight into processes ranging from knee morphogenesis[1,2]to the development of osteoarthritis (OA)[3]. Prior studies examined crosstalk among cartilage, bone, meniscus, and synovium, noting how changes in tissue structure or paracrine signaling influence joint health[4–8]. More recently, the infrapatellar fat pad (IFP) was identified as an active synovial joint tissue that contributes to joint health[9].

Several studies examined how the IFP contributes to OA risk by focusing on a range of outcomes, including changes in IFP size, magnetic resonance-detected synovitis, fibrosis, cellular composition, gene expression, and secreted proteins (reviewed in[10–13]). Notably, compared to subcutaneous fat, the IFP is more inflammatory, fibrotic, vascularized, innervated, and composed of smaller adipocytes resistant to high-fat diet-induced hypertrophy[14]. A recent single-cell analysis of synovium and IFP tissue identified a common mesenchymal progenitor cell population that gives rise to synovial lining layer fibroblasts, IFP adipocytes, and OA-associated myofibroblasts in synovium-IFP tissues[15], suggesting that synovium and intra-articular adipose tissue function in an integrated manner under basal and disease conditions.

Given the central role of unresolved inflammation in OA pathophysiology, there is a critical need to develop strategies that promote the resolution of inflammation in synovium and joint fat pads[16]. One potential strategy is to target biochemicals or signaling pathways activated by exercise therapy. The clinical benefits of exercise therapy are well documented for managing OA pain and function[17,18], although the biological mechanisms underlying these benefits and their effects on joint inflammation are not fully established.

Our goal was to determine the adaptive effect of daily wheel running exercise on metabolic remodeling and inflammation in the IFP. Biomechanical stress is a central regulator of cellular signaling across joint tissues[19,20]. At physiologic levels, cyclic tissue strain increases anti-inflammatory signaling and stress resistance pathways in multiple cells of the joint[21–23], including synoviocytes[24]. Adipocytes are highly sensitive to changes in the mechanical environment[25], and hyper-physiologic knee loading, with or without anterior cruciate ligament injury, causes IFP atrophy, fibrosis, and inflammation[26,27]. However, the effects of physiologic cyclic loading on IFP adipocyte structure and inflammation are not known. Exercise has profound effects on subcutaneous and gonadal white adipose tissue[28], including the secretion of metabolic signaling moieties (i.e., "exerkines")[29]that suppress inflammation[30]and enhance insulin sensitivity[31]. We hypothesized that voluntary wheel running exercise would induce similar benefits in synovium-IFP tissue, leading to improved metabolic regulation and reduced inflammation.

Although the long-term goal of this work is to develop strategies to mitigate OA-associated joint inflammation, the current research examined young, healthy animals so that the effect of daily exercise on IFP inflammation could first be established in non-diseased joints. Contrary to our hypothesis, we observed a transient inflammatory response in synovium-IFP tissue of uninjured knee joints following the initiation of daily exercise. Inflammation transitioned from a state of activation to resolution between 1 and 3 days of wheel running exercise and returned to pre-exercise baseline levels (or lower) by 14 days of running. The transient inflammatory response was associated with elevated $CD45^{+}Gr1^{+}$ myeloid cells (e.g., neutrophils) and oxidized phospholipids in synovial-IFP tissue after 3 days of exercise, which returned to baseline levels by 14 days of exercise. At the tissue level, IFP collagen content increased, and adipocytes transiently decreased in size. Exercise also induced orchestrated changes in synovial fluid metabolites, dominated by increased levels of amino acids, peptides, bile acids, sphingolipids, dicarboxylic acids, and straight medium chain fatty acids and decreased hydroxy fatty acids and diacylglycerols. Together, this study provides a temporal analysis of dynamic inflammatory and metabolic changes of uninjured knee joints following the initiation of daily exercise.

Methods

Animals and experimental treatments

All methods were performed in accordance with relevant guidelines and regulations and are reported in accordance with ARRIVE guidelines. We conducted all experiments following protocols approved by the Institutional Animal Care and Use Committees (IACUCs) at the Oklahoma Medical Research Foundation (OMRF) (protocols 12–47, 14–19, 17–24, 19–49, and 22–60) and Oklahoma City VA (protocol 1907-001). Animals were euthanized according to approved IACUC protocols and AVMA guidelines, which involved CO_2 asphyxiation followed by cervical dislocation to confirm death or exsanguination under isoflurane anesthesia to allow for terminal blood collection. C57BL/6J mice and $TLR4^{-/-}$ mice were purchased from The Jackson Laboratory (Bar Harbor, ME, USA) or generated from breeding colonies maintained in the OMRF vivarium. A total of 142 animals were used in these studies. Animals were group housed (≤5 animals/cage) with *ad libitum* access to chow and water in ventilated cages in rooms maintained at 22 ± 3 °C on 14 h:10 h light/dark cycles (dark phase begins at 2000, 24-hour clock). Purchased animals were habituated to the facility for 2 weeks prior to experimentation. Animals were selected for voluntary wheel running exercise treatment based

on random cage selection. Selected animals were individually housed in cages containing a 4.5-inch diameter stainless steel running wheel (MiniMiter, USA). Running activity was monitored continuously throughout the study in 1-minute intervals using an automated computer acquisition system (VitalView, USA). Non-exercised animals (i.e., "0 days exercise") were maintained in standard group-housed cages. Exercise was initiated on the appropriate date so that all animals were 14 weeks of age at the time of euthanasia in all experiments.

In the first set of experiments (cohorts 1 and 2), we studied male C57BL/6J mice to test the effect of 0-, 3-, and 14-days of wheel running exercise on IFP structure (cohort 1), inflammatory gene expression (cohort 1), and stromal vascular fraction (SVF) cell populations (cohort 2). We performed targeted follow-up studies involving 1-day exercise in male C57BL/6J mice and 3-days exercise in male C57BL/6J versus TLR4$^{-/-}$ mice. Following this first round of experiments, we performed a second round of experiments using male and female C57BL/6J mice to test the effect of 0-, 1-, 3-, and 5-days exercise and isoproterenol treatment on IFP structure (cohorts 3 and 4), inflammatory gene expression (cohort 3), and synovial fluid metabolites (cohort 3).

For experiments involving isoproterenol treatment (cohorts 3 and 4), we performed intra-articular knee injections in isoflurane anesthetized mice as previously described[27]. Briefly, we administered 2 µl of sterile saline or filter sterilized isoproterenol hydrochloride (2.5 µg/µl; cat. I6504, Sigma-Aldrich) to the right knee in a randomized, blinded manner, with the contralateral knee receiving the opposite solution. Treatments were administered between 1400 and 1600 (24-hour clock) prior to the first night of exercise. For 0-day (i.e., non-exercise) or 1-day exercise groups, animals were euthanized approximately 18 h after intra-articular treatment (i.e., 0830–1030 the following morning).

Histological and immunofluorescent analyses

Knees were dissected as previously described[32], fixed in fresh 4% paraformaldehyde (pH 7.4) for 24 h at 4 °C, and decalcified in 10% ethylenediaminetetraacetic acid (EDTA) (pH 7.2–7.4) for 14 days at 4 °C. Knees were then dehydrated in an ethanol gradient prior to paraffin embedding and sagittal sectioning. To evaluate IFP and adipocyte structure, slides were stained in saturated picric acid with 0.1% Sirius red F3B (VWR), washed in 0.5% acetic acid, and counterstained with 0.5% Harris' hematoxylin (VWR). Intercondylar mid-IFP sections were captured at 4X and 10X magnification using a Nikon E200 microscope equipped with a DS-Fi3 digital camera. We used Fiji/ImageJ2 software (v2.9.0/1.54b) with the Adiposoft plugin to automatically measure adipocyte cross-sectional area[33]. To improve accuracy, cell diameter limits were pre-set at 10–200 µm, and analyses were manually inspected and edited for cell exclusion/inclusion. Relative collagen content was evaluated based on epipolarized imaging of picrosirius red stained IFP sections, as previously described[34]. Investigators were blinded to sample groups assignments for histological analyses.

Oxidized phospholipids were detected by E06 antibody immunostaining[35]. Tissue slides were heated to 60 °C for 30 min, deparaffinized in xylene, rehydrated in a graded ethanol series, and washed in distilled water. Antigen retrieval was performed by microwaving slides in sodium citrate buffer (10mM Sodium Citrate, 0.05% Tween 20, pH 6.0) for 5 min, cooling at room temperature for 20 min, and washing in 1× phosphate buffered saline (PBS). Nonspecific binding was blocked using rabbit serum (Jackson Research Labs, #011-000-120, 1:100 in PBST [0.5% Tween20 in 1× PBS]). Slides were incubated with E06 monoclonal antibody (Avanti Polar Lipids Inc, Lot 330001 S-100UG-A-026, 1:250 in blocking solution) for 2 h at room temperature and washed in PBST. Slides were then incubated with Rhodamine (TRITC)-conjugated AffiniPure rabbit anti-mouse IgM secondary antibody (Jackson Research Labs, #315-025-049, 1:400) for 1 h at room temperature and washed in PBST. Tissue sections were counterstained with DAPI Vectashield mounting media, and sections were imaged using a Zeiss 710 confocal microscope.

Gene expression analyses

As previously described[27], synovium-IFP tissue was dissected immediately after death, flash-frozen in liquid nitrogen and stored at −80 °C. RNA was isolated from frozen tissue using a TissueLyser (Qiagen), extracted with TRIzol followed by chloroform, and purified using a Clean and Concentrator kit (Zymo Research). 200 ng RNA from each sample was reverse-transcribed into cDNA using an RT2 First-Strand kit (Qiagen). In initial experiments, synovium-IFP gene expression was measured using a custom designed RT2 Profiler PCR Array (CAPM13071D; Qiagen) according to manufacturer instructions. The custom array included 3 reference genes (*Hprt*, *Gapdh*, *Actb*), positive and negative control wells, and 42 inflammation-associated target genes (**Supplemental Table 1**). Additional custom arrays were utilized for analysis of 1-day exercise samples (**Supplemental Table 2**) and TLR4$^{-/-}$ samples (**Supplemental Table 3**). Samples were analyzed on a CFX96 thermocycler (Bio-Rad), and gene expression was quantified relative to the geometric mean of the reference gene critical threshold values. In later experiments comparing exercise duration, isoproterenol treatment, and biological sex, synovium-IFP gene expression was measured by qPCR using a custom DELTAgene Assay that included 90 target genes selected for their role in adipose-tissue homeostasis, fibrosis, inflammation, nociception, and cell adhesion (see[27] for additional details). All samples were run on a single microfluidic 96.96 IFC array using a BioMark HD instrument.

Flow cytometry analyses

Synovium-IFP stromal vascular fraction cells were isolated and prepared for evaluation by flow cytometry as previously described[34], with minor modification. IFP samples from both knees were digested at 37 °C for 30 min on an orbital shaker in 1 ml Dulbecco's modified Eagle's medium (DMEM) containing 25 µg/ml Liberase TH (Roche). Inguinal region subcutaneous fat was collected from a subset of animals for tissue-specific comparison. Tissue was homogenized with gentle pipetting, and the mixture was filtered (70 µm) and centrifuged at 1500 RPM for 10 min at 4 °C. Cell filtrate was incubated in 1× red blood cell lysis solution for 1 min at room temperature followed by a DMEM wash and centrifugation. Freshly isolated cells were resuspended in fluorescence-activated

cell sorting buffer (1× PBS with 5% fetal bovine serum), counted (123count eBeads, eBioscience), and labeled for 15 min on ice with a cocktail of fluorochrome-conjugated monoclonal antibodies: CD45.2 (clone 104, BD Horizon #560697 – V450), CD3ε (145-2C11, BioLegend #100347 - PETxRd), CD11c (N418, BioLegend #117309 - APC), CD19 (6D5, BioLegend #115529 – APCCy7), CD140 (APA5, eBioscience #12–1401 - PE), CD206 (C068C2, BioLegend #141719 – PECy7), F4/80 (BM8, BioLegend #123127 – PercpCy5.5), and Ly-6 C/Ly-6G (Gr-1) (RB6-8C5, BioLegend #108443 – BV711). Compensation for each fluorochrome was performed with BDCompBead Anti-Rat and Anti-Hamster Ig, K/negative control compensation particles (BD Biosciences, #552845) and single stain controls. Cell viability was determined using Zombie Aqua cell viability dye (BioLegend, catalog #423101). Data were acquired on a BD LSR II flow cytometer and analyzed with FlowJo software (Tree Star). To obtain sufficient cell numbers for analysis, cells were combined from synovium-IFPs of 6 animals per experimental group, and experiments were repeated 3–6 times for each group.

Synovial fluid metabolomic analyses

Synovial fluid was collected for metabolomic analysis as previously described[27,36] and stored at −80°C until analysis. Samples were shipped overnight on dry ice to Metabolon (Morrisville, NC, USA) and processed according to their standard pipeline for Global Metabolomic Profiling Analysis (details in[27]). Raw data were extracted, peak-identified, and processed for quality-control using Metabolon's hardware and software. Compound identification was based on comparison to authenticated standard library entries within a narrow retention time/index window, accurate mass to charge ratio (m/z) +/- 10 ppm, and chromatographic data including MS/MS forward and reverse scores between the experimental data and authentic standards. The analysis identified 202 named biochemicals within Metabolon's authenticated standard library (see[27] for detailed listing), which were detected in nearly all samples (mean = 93.6%, median = 100%). Peak area data were normalized to extracted volume and then median scaled. Any undetected values (< 6.5% of data set) were imputed with sample set minimums on a per biochemical basis.

Statistical analyses

Animal sample sizes for histomorphology, gene expression, and flow cytometry analyses were based on our prior research examining the effect of a high fat diet on the IFP[34]. No animals died during experiments, although some analyses had reduced group sizes due to technical issues with sample processing, as indicated in **Supplemental Table 5**. The effect of exercise duration was evaluated by one-way ANOVA. Data that did not meet test assumptions for normality or homoscedasticity, even after log transformation, were analyzed using the Kruskal-Wallis test. Analyses involving more than one effect (e.g., exercise duration, biological sex, isoproterenol treatment) were analyzed by repeated measures two-way ANOVA, mixed model analysis, or generalized linear model analysis as indicated in figure legends and **Supplemental Table 5**. Multiple comparison-adjusted post-hoc tests to identify individual group differences are also specified in figure legends and **Supplemental Table 5**. Hierarchical clustering analyses were performed to identify genes and metabolites that shared similar expression patterns in response to exercise. Gene and metabolite data were standardized by subtracting the mean and dividing by the standard deviation, and Ward's minimum variance method was used to calculate cluster distances. Additional statistical details are provided in figure legends. All statistical analyses were performed with Prism 10.2.2 (GraphPad Software, Inc) or JMP Pro 16.0.0 (SAS Institute, Inc).

Results

Exercise-induced IFP structural remodeling

We observed that 3-day and 14-day exercise groups ran similar daily distances (3-day exercise total distance: 15.46 ± 4.16 km; 14-day exercise total distance during last 3 days: 18.49 ± 4.11 km; mean ± SD; $p = 0.28$, 2-tailed t-test). Thus, differences between 3- and 14-days exercise are not likely due to differences in the intensity of wheel running exercise. We began by comparing the effect of 3 and 14 days of wheel running versus 0 days of running (i.e., standard cage activity) on IFP histomorphology. The average IFP cross-sectional area (CSA) of the 3-day exercise group was 21% smaller than the 0-day group, although this difference was not significant ($p = 0.19$) (Fig. 1A). We next investigated the effect of exercise duration on the CSA of IFP adipocytes. While the average per animal adipocyte CSA was similar across all groups ($p = 0.40$), the within group coefficient of variation was twice as large in the 3-day versus 0-day condition (21.0% vs. 10.6%, respectively) (Fig. 1B). A histogram frequency analysis of all evaluated adipocytes indicated that the 3-day exercise group had a higher frequency of adipocytes with CSAs < 200 μm^2 and a smaller mean CSA compared to 0- and 14-day groups (Fig. 1B). IFP collagen content was not significantly altered by exercise, although there was a trend for greater collagen with 3- versus 0-days exercise ($p = 0.0853$) (Fig. 1C). In addition, the coefficient of variation of IFP collagen content in 3- and 14-day exercise groups (29.6% and 35.0%, respectively) was greater than the 0-day condition (20.2%).

Exercise duration and IFP-synovium gene expression

We next evaluated the effect of exercise duration on the expression of genes involved in inflammation and fibrosis. Two-way hierarchical clustering analysis of standardized gene expression values showed that 0- and 14-day exercise conditions were more similar than the 3-day exercise condition (Fig. 2A). The analysis also grouped genes into five major clusters (C1-C5) based on exercise-dependent expression patterns (Fig. 2B). Notably, half of all genes aligned with cluster 3 (C3), which was characterized by elevated expression at day-3 versus days 0 and 14. One-third of C3-associated genes were significantly altered by exercise ($p < 0.05$). These genes primarily included key pro- and anti-inflammatory mediators associated with myeloid cells (e.g., *Il1b*, *Ccl2*, *Ccr2*, *Mrc1*, *Il1rn*, *Emr1*, and *Itgb2*) (Fig. 2C). These results strongly suggest that 3 days of running wheel exercise induced synovium-IFP inflammation, which resolved by 14 days of exercise.

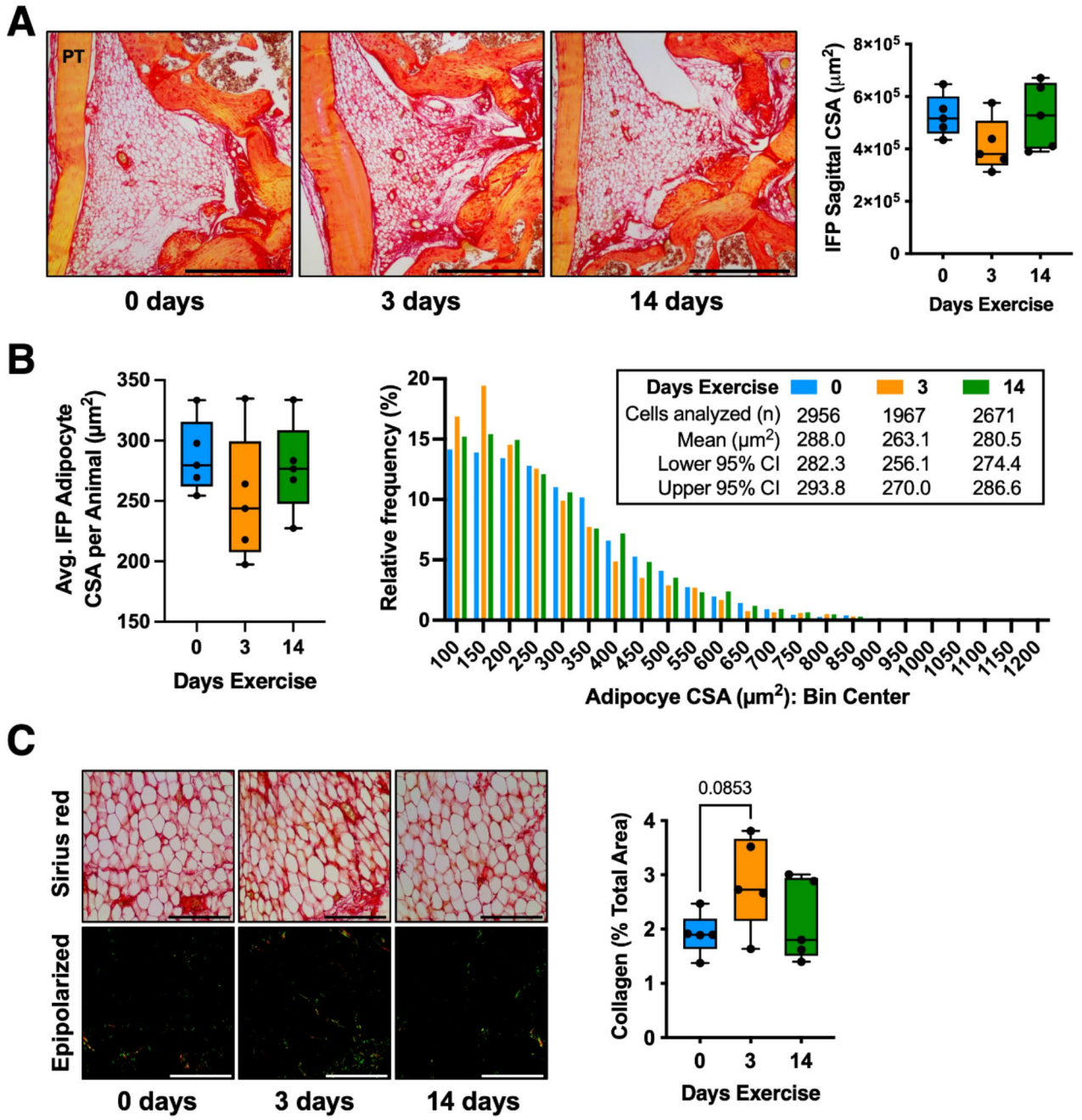

Fig. 1. Effect of wheel running on infrapatellar fat pad (IFP) structure. (**A**) Representative Sirius red-stained mid-sagittal paraffin sections of the IFP from male mice following 0, 3, or 14 days of voluntary wheel running. PT = patellar tendon; scale bar = 500 μm. Data points represent the mid-sagittal cross-section area (CSA) of the IFP ($n = 5$ per group). Boxplot shows the 25th to 75th percentiles, horizontal line indicates the median, and whiskers denote maximum and minimum values. (**B**) Boxplot and histogram frequency analysis of individual adipocyte CSA across running exercise conditions. Boxplot data points represent the average IFP adipocyte CSA per animal, whereas histogram analysis is based on the total cells analyzed per exercise condition. (**C**) Brightfield (top) and epipolarized ultraviolet light (bottom) representative images of Sirius red-stained sections used for collagen analysis; scale = 100 μm. Yellow-green pixels from epipolarized images were quantified as a percent of the image area to determine the relative collagen content. Boxplot graphs analyzed by one-way ANOVA, with post-hoc paired comparisons between 0 vs. 3 and 0 vs. 14 days exercise evaluated by Dunn's multiple comparisons test ($p \leq 0.10$ shown).

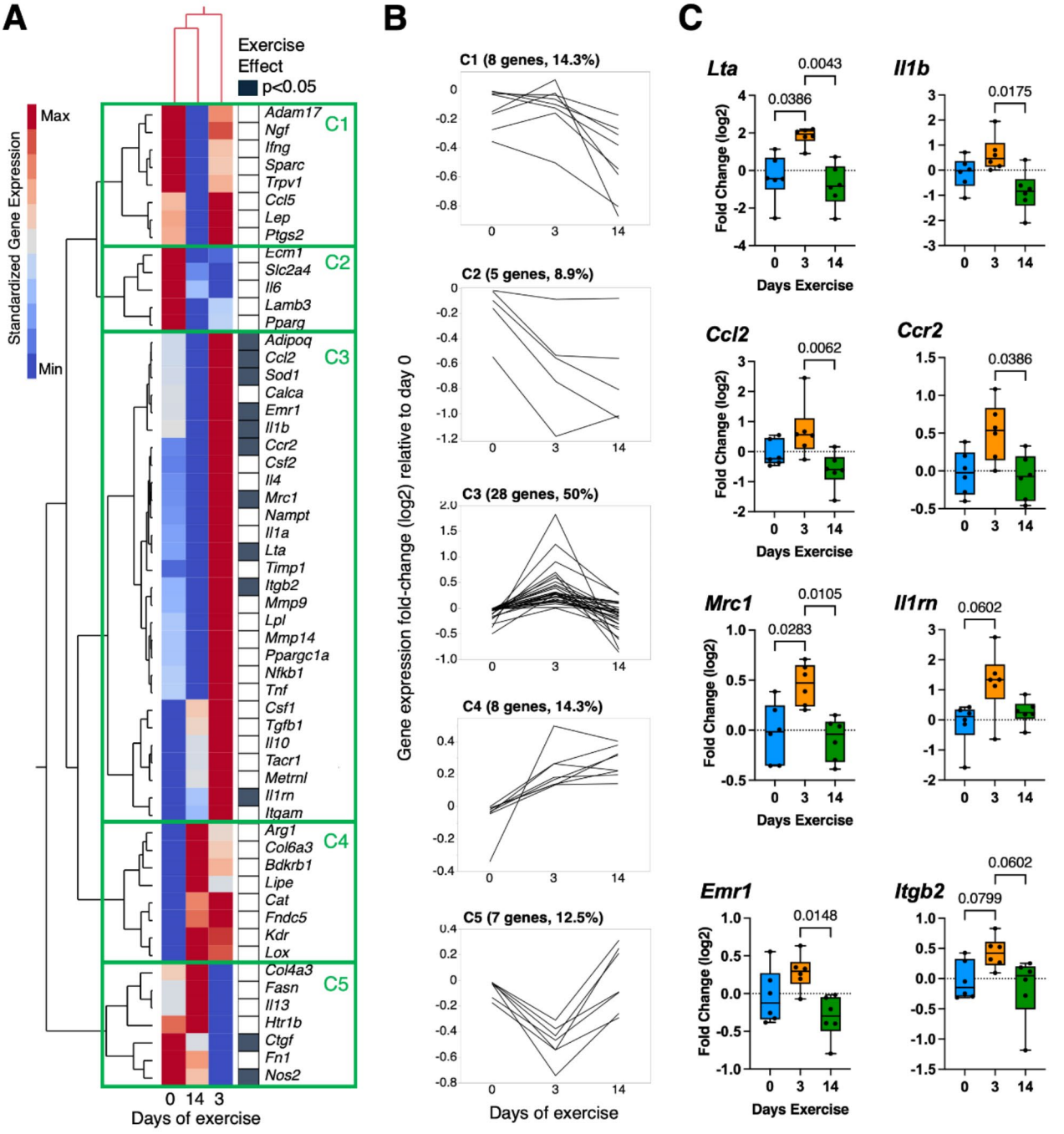

Fig. 2. Wheel running exercise induces transient inflammatory gene expression in synovium-IFP tissue. (**A**) 2-way hierarchical clustering analysis was used to identify patterns in gene expression across experimental groups. Heatmap color legend signifies standardized gene expression values calculated by subtracting the mean of log2-transformed values and dividing by the standard deviation. Columns represent mean values per experimental group, and rows show the targeted genes. Note that 0- and 14-day exercise conditions clustered together in the first and second columns. Filled cells in right-hand column indicate genes significantly altered by exercise (Kruskal-Wallis test; $p < 0.05$). (**B**) Line graphs of gene expression fold-change (log2) expressed by days of exercise and grouped by heatmap cluster (C1 – C5). Half of all target genes grouped in C3, characterized by elevated gene expression in the 3-day exercise group. (**C**) Boxplots of select inflammation-associated genes from C3 that were altered by exercise show the 25th to 75th percentiles; horizontal line indicates the median, and whiskers denote maximum and minimum values ($n = 6$ per group). Data analyzed by Kruskal-Wallis test, with post-hoc paired comparisons evaluated by Dunn's multiple comparisons test ($p \leq 0.10$ shown).

Exercise duration and IFP-synovium stromal vascular fraction cell populations

Stromal vascular fraction cells were isolated from synovium-IFP tissue of animals following 0, 3, and 14 days of wheel running exercise. Exercise significantly altered the relative number of $CD45^+$cells ($p = 0.0405$) and $CD45^+Gr1^+$cells ($p = 0.0316$), consistent with an acute neutrophil infiltration that fully resolved by 14 days of exercise (Fig. 3A, B). Between 3 and 14 days of exercise, the relative number of $CD45^+Gr1^-$ cells increased, particularly $F4/80^+$ macrophages that expressed high levels of CD206 (Fig. 3B). Exercise did not substantially alter other lymphoid ($CD19^+$, $CD3^+$), myeloid ($CD11c^+$), or fibro/adipogenic progenitor ($CD45^-CD140^+$) cell

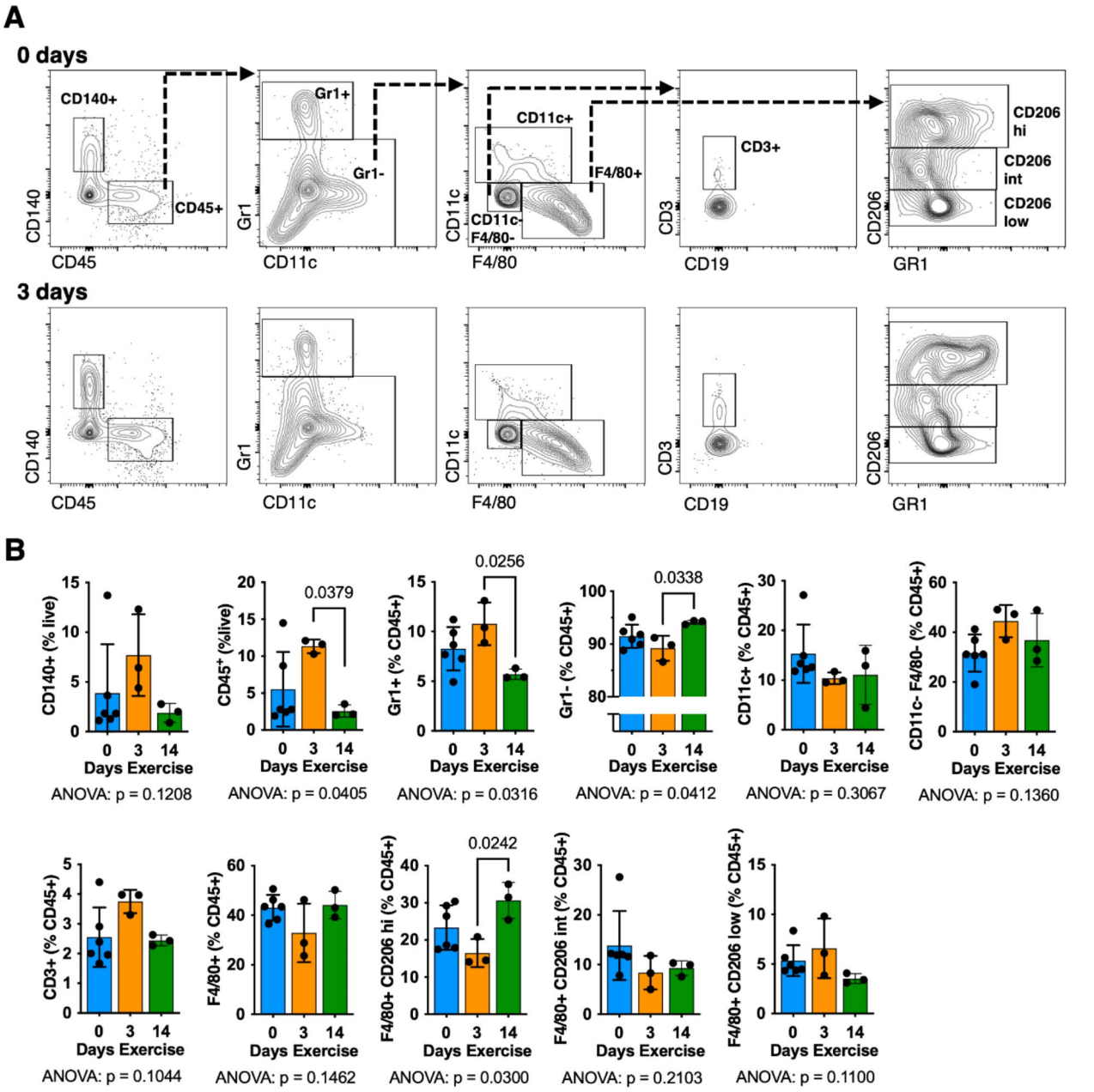

Fig. 3. Effect of wheel running exercise on synovium-IFP cell populations. Stromal vascular fraction cells were isolated from animals following 0, 3, or 14 days of voluntary wheel running. Cells were pooled from synovium-IFP tissue collected from both knees of six animals per flow cytometry experiment for each group. Experiments were repeated 3–6 times, as shown by individual data points. Thus, total animals per experimental group are $n = 36$ (0 days) and $n = 18$ (3 days, 14 days). Note that statistics are based on replicate experiments ($N = 3$–6). (**A**) Representative contour plots and gating strategy for 0- and 3-days exercise. (**B**) Bar graphs showing mean ± SD of indicated cell populations. Results analyzed by one-way ANOVA, with post-hoc paired comparisons evaluated by Tukey's multiple comparisons test ($p \leq 0.10$ shown). A comparison of synovium-IFP and subcutaneous fat derived stromal vascular fraction cell populations is provided in Supplemental Table 4.

populations. For additional context, we compared cells isolated from synovium-IFP tissue to those isolated from subcutaneous inguinal fat (**Supplemental Table 4**). Exercise altered the population of $CD45^{+}Gr1^{+}$ cells and $CD206^{high}$ macrophages similarly in both tissues despite the relative number of $CD45^{+}$ immune cells and $F4/80^{+}CD206^{low}$ macrophages being greater in subcutaneous fat compared to synovium-IFP tissue (**Supplemental Table 4**).

Exercise-induced phospholipid oxidation and acute inflammation

Based on gene expression and flow cytometry results indicating a transient pro-inflammatory effect of exercise on synovium-IFP tissue, we evaluated the effect of exercise on phospholipid oxidation using the murine monoclonal antibody E06. Oxidized phospholipids are common features of tissue injury, serving as damage-associated molecular patterns (DAMPs) to stimulate innate immune activity by macrophages and dendritic cells[37]. Although it is not known if wheel running exercise causes synovium-IFP tissue damage, wheel running (< 14 days) has been shown to induce skeletal muscle oxidation and remodeling, which involves a cycle of degeneration, necrosis, and phagocytosis[38]. We observed increased E06 staining in synovium-IFP with 3 days exercise compared to non-exercise control animals ($p = 0.0489$), particularly along the anterior IFP surface (Fig. 4A, B). Oxidized phospholipids promote pro-inflammatory signaling in part through toll like receptor 4 (TLR4)[37]; therefore, we compared the effect of 3 days wheel running exercise on IFP structural remodeling and inflammation in WT and $TLR4^{-/-}$ mice (**Supplemental Fig. 1**). IFP adipocyte CSA was larger in $TLR4^{-/-}$ versus WT mice, and there was a trend for less IFP collagen content in $TLR4^{-/-}$ versus WT mice. Contrary to expectations, pro-inflammatory genes were more highly expressed in $TLR4^{-/-}$ versus WT mice (e.g., *Tnf*,

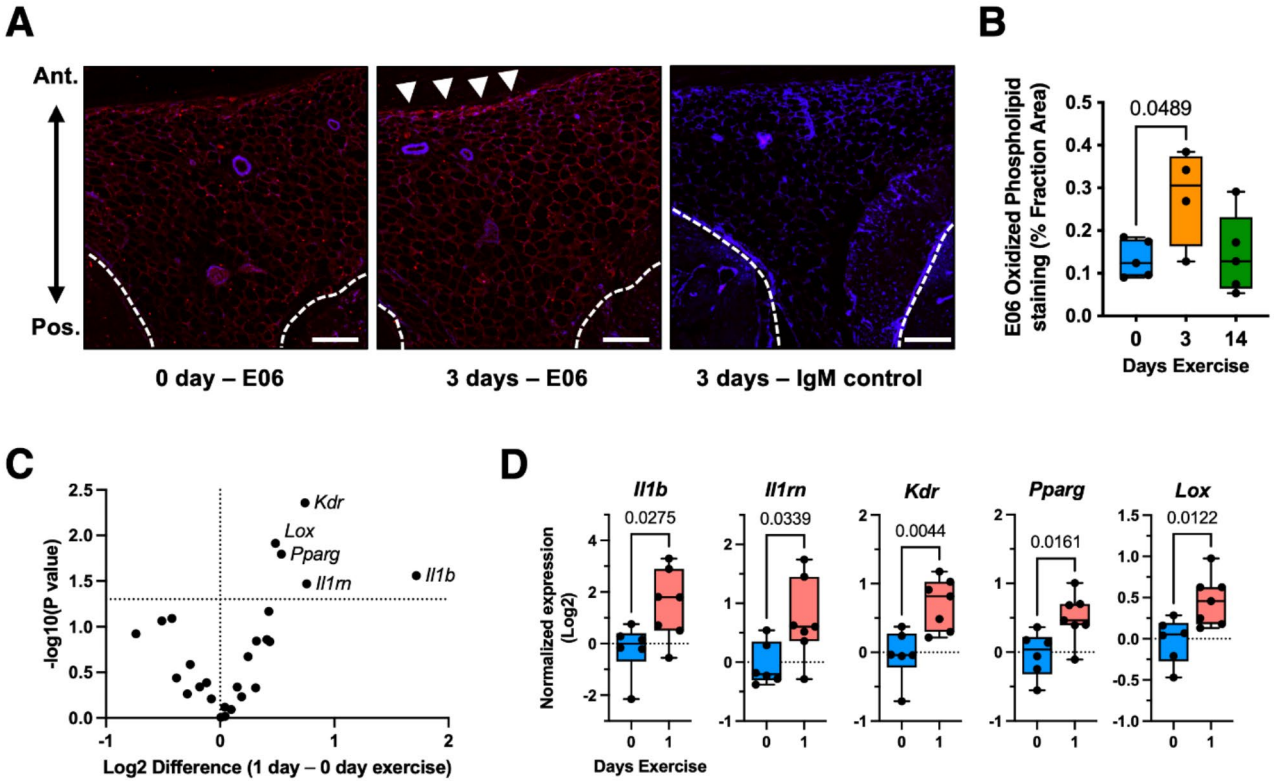

Fig. 4. Acute pro-inflammatory effects of wheel running exercise on synovium-IFP tissue. (**A**) Phospholipid oxidation was evaluated as a potential mediator of exercise-induced inflammation. Mid-sagittal IFP sections were stained with the murine monoclonal antibody E06, which specifically binds to the phosphorylcholine head group of oxidized but not native phospholipids. Representative images shown for E06 (0- and 3-days exercise) and IgM control (3-day exercise) antibody staining. White arrowheads indicated elevated E06 staining along the anterior IFP surface. Dashed white lines indicate the posterior boarder of the IFP. Scale bar = 100 µm. (**B**) Boxplot graph of E06 antibody staining, expressed as a percentage of the IFP cross-sectional area. Boxplot shows the 25th to 75th percentiles, horizontal line indicates the median, and whiskers demonstrate maximum and minimum values ($n = 4$–5 per group). Data analyzed by one-way ANOVA, with post-hoc paired comparisons between 0 vs. 3 and 0 vs. 14 days exercise evaluated by FDR method of Benjamini and Hochberg ($p \leq 0.10$ shown). (**C**) Effect of 1-day exercise on synovium-IFP gene expression was evaluated by unpaired t test ($p < 0.05$) and visualized by volcano plot. Analysis included 26 target genes related to inflammation, fibrosis, and adipose tissue homeostasis. (**D**) Boxplots comparing differentially expressed genes in the 0- vs. 1-day exercise groups ($n = 6$–7 per group). Values were normalized to 0-day exercise, log2 transformed, and analyzed by two-tailed unpaired t test.

Il1a, *Il1b*, *Ccl2*, and *Ccr2*), indicating that TLR4 protects against exercise-induced synovium-IFP transient inflammation.

To better understand the time course of exercise-induced inflammation, we evaluated the effect of 1 day of exercise on synovium-IFP gene expression in WT mice. After 1 day, the expression of *Il1b* and *Il1rn* were upregulated 3.3-fold [1.2, 9.2] and 1.7-fold [1.0, 2.7] (mean [95%CI]), respectively, compared to non-exercised mice (Fig. 4C, D). For comparison, after 3 days of exercise (Fig. 2C), *Il1b* expression was 1.7-fold greater and *Il1rn* was 2.6-fold greater than 0-day exercise animals. These data indicate that exercise-induced *Il1b* expression diminished from 1 to 3 days of exercise, whereas the expression of *Il1rn*, an anti-inflammatory mediator, increased during this period. One day of exercise also upregulated the expression of genes associated with angiogenesis (*Kdr*), adipogenesis (*Pparg)*, and collagen crosslinking (*Lox)* (Fig. 4C, D).

IFP structural remodeling: Sex comparison and isoproterenol treatment

Based on our observations of a transient inflammatory response to wheel running exercise, we conducted a follow-up study focused on the first 5 days of exercise. Using both male and female mice, we evaluated the effect of a pre-exercise intra-articular injection of isoproterenol, which is a β-adrenergic receptor (βAR) agonist that stimulates adipose tissue lipolysis and suppresses the activity of pro-inflammatory macrophages[39,40]. Our previous study of synovial fluid metabolites indicated that exercise stimulated catecholamine biosynthesis[41], suggesting that catecholamines may counteract the pro-inflammatory response to exercise. We hypothesized that intra-articular isoproterenol treatment prior to initiating exercise would induce IFP lipolysis and suppress the transient inflammatory response to exercise.

In non-exercised animals (day 0), neither sex nor isoproterenol treatment altered the average IFP adipocyte CSA (Fig. 5A, B). When 0-, 1-, 3-, and 5-day exercise conditions were considered together, there was still no effect of sex or isoproterenol treatment on average IFP adipocyte CSA or IFP collagen content (**Supplemental Table 5**). However, as previously observed for male mice, 3 to 5 days of exercise reduced the average IFP adipocyte CSA in both male and female mice ($p = 0.0053$; Fig. 5A, C). We also observed that 5 days of exercise increased the percent collagen content in the IFP ($p = 0.034$; Fig. 5A, D).

IFP-synovium gene expression: Dynamic changes during short-term exercise

We next evaluated the effect of exercise duration, sex, and isoproterenol treatment on the expression of genes involved in inflammation, fibrosis, and adipose tissue homeostasis. Exercise altered the expression of nearly half of the tested genes (40/81), which greatly exceeded differences due to sex (9/81) or isoproterenol treatment (4/81) (**Supplemental Table 6**). Based on the predominant effect of exercise on synovium-IFP gene expression, we performed a two-way hierarchical clustering analysis of standardized gene expression values across 0-, 1-, 3-, and 5-days exercise (Fig. 6A). The analysis showed that 0- and 1-day exercise conditions were more similar than 3- and 5-day exercise conditions, and it also identified six clusters of exercise-dependent gene expression patterns (C1-C6). Most genes in clusters 2, 5, and 6 were significantly altered with exercise (Fig. 6A), and the genes in these clusters also underwent the greatest magnitude changes with exercise (Fig. 6B). 3- and 5-days of exercise upregulated the expression of genes in cluster 2, which included genes associated with fibrosis (*Col1a1*, *Col3a1*, *Col6a3*, *Fn1*), matrix remodeling (*Mmp14*), and tissue repair macrophages (*Csfr1*, *Adgre1*, *Mrc1*, *Trem2*, *Tgfb1*) (Fig. 6A-C). In contrast, 3 to 5 days of exercise downregulated the expression of genes in clusters 4 and 5, which included genes associated with adipose tissue and metabolism (*Cd36*, *Lep*, *Calca*, *Foxa2*, *Ffar4*, *Klf15*, *Dgat1*) (Fig. 6A-C). Genes in cluster 6 were acutely upregulated after 1 day of exercise and subsequently downregulated to baseline levels (or lower) by day 5 of exercise (Fig. 6A-C). Notably, cluster 6 was primarily composed of pro-inflammatory genes (e.g., *Tnf*, *Il1b*, *Ccl2*, *Ccr2*, *Nlrp3*, *Cxcl1*, *Ccl3*, *Osm*, *Cd14*).

Synovial fluid metabolomics: Dynamic changes during short-term exercise

We evaluated the effect of exercise duration, sex, and isoproterenol treatment on 202 synovial fluid metabolites whose identities were validated by authenticated standards. Similar to the results for synovium-IFP gene expression, exercise had a much greater effect on synovial fluid metabolite levels compared to sex or isoproterenol treatment. 150 metabolites were significantly altered by exercise compared to 27 metabolites and 4 metabolites altered by sex and isoproterenol, respectively ($p < 0.05$, **Supplemental Table 7**). Sex differences were most notable in metabolites that varied the most with exercise based on Variable Importance in Projection (VIP) Scores, which included relatively more carbohydrate, energy, and nucleotide super pathway metabolites in females and relatively more lipid and xenobiotics super pathway metabolites in males (**Supplemental Fig. 2**). We next performed a two-way hierarchical clustering analysis of standardized synovial fluid metabolite values across 0-, 1-, 3-, and 5-days exercise. The analysis showed that 3- and 5-days exercise were more alike than 0- and 1-day exercise, and it identified 5 exercise-induced patterns of change in synovial fluid metabolites (C1-C5) (Fig. 7A).

Cluster 1 (C1), the largest cluster, was characterized by increasing metabolite levels following 3 to 5 days of exercise. To characterize these changes, we compared the relative proportion of total detected metabolites in each metabolic pathway (Fig. 7B) to those present within the cluster (Fig. 7C). C1 metabolites were enriched for amino acids and peptides and included proportionate contributions of cofactors and vitamins, energy, nucleotide, and xenobiotic metabolites (Fig. 7C). Cluster 2 (C2) was composed of metabolites similar to C1, and like C1, the metabolites increased with exercise, although the levels peaked sooner at 1 to 3 days of exercise. Cluster 3 (C3) was the smallest cluster with 13 metabolites. These metabolites were only transiently elevated after 1 day of wheel running and included 3-hydroxybutyrate, butyrate/isobutyrate (4:0), and nicotinamide riboside (Fig. 7C, **Supplemental Table 7**). Cluster 4 (C4) also contained a small number of metabolites, with few significantly altered by exercise. Cluster 5 (C5) contained 34 metabolites. These metabolites decreased with exercise, and they were enriched for carbohydrates and lipids and diminished in amino acids and peptides (Fig. 7C). Most of the downregulated carbohydrates mapped to pentose metabolism sub-pathway, while downregulated lipids

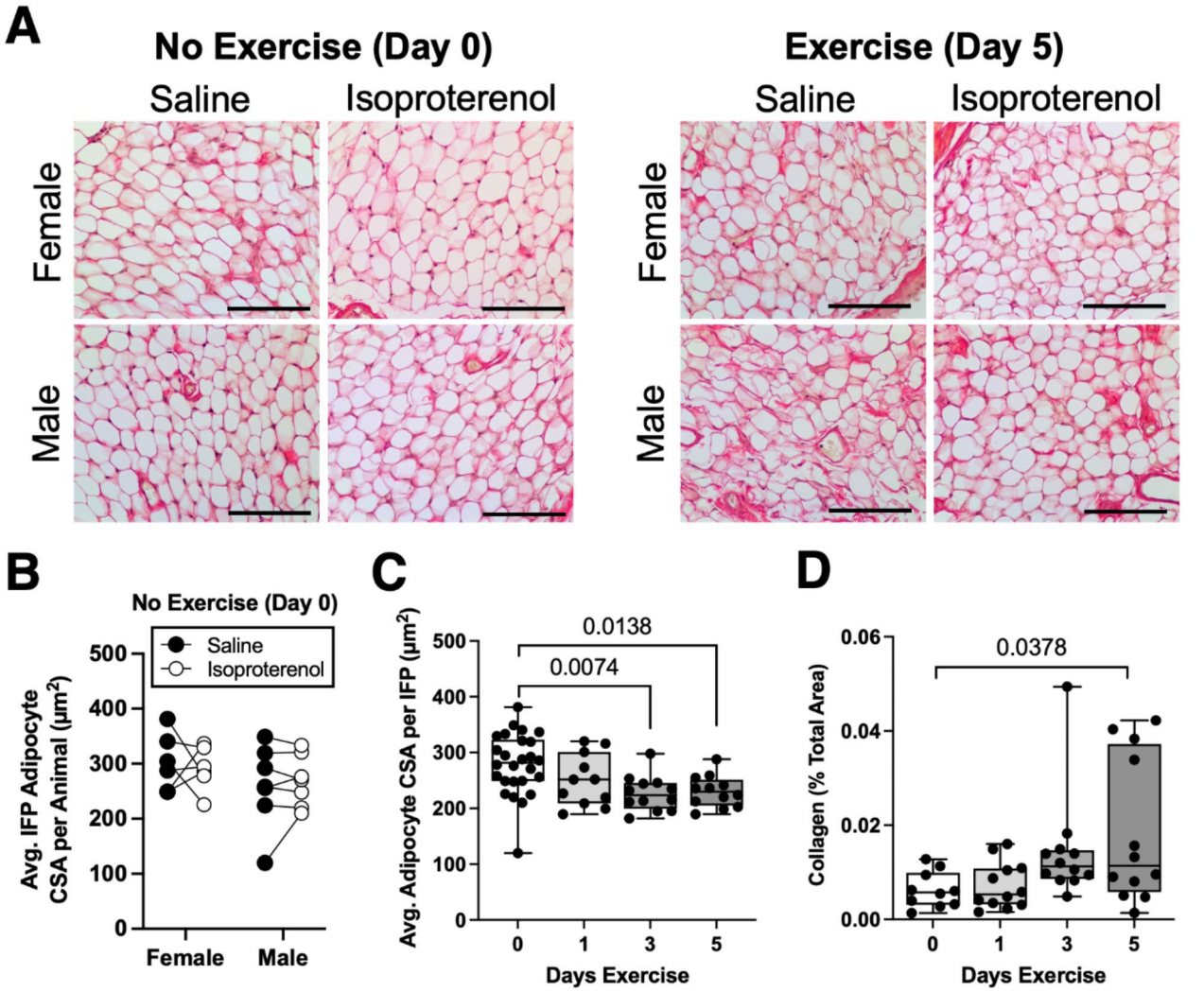

Fig. 5. Short-term wheel running alters infrapatellar fat pad (IFP) structure independent of biological sex or isoproterenol treatment. (**A**) Representative Sirius red-stained mid-sagittal paraffin sections of IFP tissue from female and male mice following 0 or 5 days of voluntary wheel running after intra-articular saline or isoproterenol treatment. Scale bar = 100 μm. (**B**) Paired within-animal analysis of average adipocyte cross sectional area (CSA) from contralateral IFPs 18 h following intra-articular treatment with saline or isoproterenol. Data analyzed by two-way repeated measures ANOVA ($p > 0.20$ for all factors). (**C**) Boxplot of the average adipocyte CSA per IFP across short-term running exercise durations (0, 1, 3, and 5 days). Data points include separate male and female animals as well as saline and isoproterenol treated IFPs from contralateral knees of the same animals. Data were analyzed using a Mixed Model analysis, with exercise duration, treatment, and sex as "Fixed Effects" (including interaction terms) and animal ID as a "Random Effect" to account for correlative data obtained from the same animal. Only exercise duration had a significant effect ($p = 0.0053$). Post-hoc paired comparisons were evaluated by Dunnett's test ($p \leq 0.10$ shown). (**D**) Boxplot of yellow-green pixels from epipolarized Sirius red-stained sections quantified as a percent of the image area to determine the relative collagen content, compared across short-term running exercise durations (0, 1, 3, and 5 days). Boxplot shows the 25th to 75th percentiles, horizontal line indicates the median, and whiskers demonstrate maximum and minimum values. Data analyzed as described in panel (C). Only exercise duration had a significant effect ($p = 0.034$).

included hydroxy fatty acids and diacylglycerols. Overall, exercise induced distinct longitudinal trajectories in different classes of synovial fluid metabolites, suggestive of an orchestrated temporal effect of exercise on joint metabolism.

Exercise-induced temporal changes in synovial fluid lipids

Given the role of lipids as metabolic substrates, signaling molecules, and mediators of inflammation, we further examined the 47 metabolites assigned to the Lipids superpathway to evaluate the effect of exercise on changes in specific sub-classes of synovial fluid lipids. We began by performing a principal component analysis (PCA) of

synovial fluid lipids as a function of exercise duration (days 0 to 5) (Fig. 8A). The PCA plot showed substantial separation between 0- and 1-day samples and 3- and 5-day samples along principal component 1 (PC1). We next compared the contribution to PC1 for each synovial fluid lipid, which was categorized by color and symbol based on Metabolon sub-pathway assignments (Fig. 8B, **Supplemental Table 7**). Lipids that positively contributed to PC1 were increased with exercise. These upregulated lipids included various types of dicarboxylic and hydroxy fatty acids (2-hydroxysebacate, suberate, azelate, sebacate), straight chain fatty acids (laurate, caprylate), bile acids (cholate, taurocholate, taurochenodeoxycholate), and sphingolipids (phytosphingosine, palmitoyl sphingomyelin, N-stearoyl-sphinganine) (Fig. 8C). In contrast, lipids that negatively contributed to PC1 were decreased with exercise. These downregulated lipids included dicarboxylic and hydroxy fatty acids (3-hydroxyadipate, 2R,3R-dihydroxybutyrate, 13-HODE + 9-HODE, 3-hydroxysuberate) and diacylglycerols (diacylglycerol [16:1/18:2, 16:0/18:3], palmitoyl-linoleoyl-glycerol, oleoyl-linoleoyl-glycerol, linoleoyl-linoleoyl-glycerol) (Fig. 8D).

Discussion

This study provides the first description of a transient inflammatory response in synovium-IFP tissue of uninjured knee joints following the initiation of daily exercise. Inflammation transitioned from a state of activation to resolution between 1 and 3 days of wheel running exercise and returned to pre-exercise baseline levels (or lower) by 14 days of running. The transient inflammatory response was associated with elevated $CD45^{+}Gr1^{+}$ myeloid cells (e.g., neutrophils) and oxidized phospholipids in synovial-IFP tissue after 3 days of exercise, which returned to baseline levels by 14 days of exercise. At the tissue level, IFP collagen content increased, and adipocytes transiently decreased in size. Moreover, within the first 5 days of exercise, synovial fluids underwent orchestrated changes dominated by increased levels of amino acids, peptides, bile acids, sphingolipids, dicarboxylic acids, and straight medium chain fatty acids and decreased hydroxy fatty acids and diacylglycerols. Taken together, these findings reveal the temporal dynamics of exercise-induced changes in joint metabolism, inflammation, and IFP remodeling.

Previous research on how exercise affects synovial joint inflammation has examined changes following either single acute bouts of exercise[42–44]or multi-week exercise training sessions[45,46]. In young, healthy, physically active adults, 30 min of treadmill running moderately reduced synovial fluid GM-CSF compared to baseline values without altering 10 other evaluated cytokines[43]. In older women with knee OA, 40 min of knee extension exercise increased intra-articular and synovial IL-10 levels compared to non-exercise controls[42]. Thus, immediately following an acute bout of exercise, the limited available data indicates an anti-inflammatory effect of exercise within the joint. However, whether similar benefits extend to a longer follow-up period is uncertain. A recent secondary analysis of a 12-week exercise therapy randomized controlled trial in OA patients reported that exercise reduced joint pain without altering MRI-assessed knee synovitis[47]. Similarly, a recent meta-analysis of 12 randomized controlled trials testing exercise-therapy interventions ranging from 4 to 24 weeks in duration reported that exercise therapy was associated with non-significant reductions in serum C-reactive protein, TNF, and soluble TNF receptors 1 and 2[45]. Thus, while exercise-based therapy is a core component of current clinical guidelines for treating knee OA[48,49], it is not clear if exercise improves OA pain by lowering inflammation. Moreover, a recent critical assessment has questioned the strength of evidence supporting a causal relationship between exercise and knee OA pain relief[50]. One reason for this critique is an insufficient mechanistic understanding of how specific types of exercise provide OA pain relief[50].

Exercise exerts broad local and systemic effects on tissue structure and organ physiology. The breadth and complexity of these responses and adaptations are thought to underlie the health-promoting benefits of exercise[51], although these same attributes create challenges for causal mechanistic analyses of how exercise improves chronic disease conditions. In recognition of this complexity, recent collaborative efforts have focused on building comprehensive, time-dependent molecular maps that document the effect of exercise on blood and other tissues in healthy animal models and humans[52,53]. We believe that similar efforts are needed for synovial joint tissues, such as the IFP, where the temporal effects of exercise are poorly understood. For example, understanding how inflammation resolves following the initiation of a daily exercise routine may provide a tractable model for identifying biological targets that promote the resolution of inflammation in OA joints, like what has been proposed for skeletal muscle diseases[54].

We recently reported that intra-articular treatment with the β-AR agonist isoproterenol reduced inflammation in female mice with post-traumatic knee OA[27]. Given the upregulation of catecholamines with exercise, we hypothesized that intra-articular isoproterenol treatment prior to wheel running exercise would suppress the initial pro-inflammatory response to exercise. However, we observed negligible effects of isoproterenol treatment on IFP structure, synovium-IFP gene expression, or synovial fluid metabolites. Thus, the results do not support our hypothesis. Moreover, when compared to our prior findings of an anti-inflammatory effect of isoproterenol treatment in female mice with post-traumatic knee OA[27], the current results suggest that injury sensitizes synovial joints to β-adrenergic signaling. OA changes the cellular populations and signaling networks within synovium-IFP tissue, especially with regards to adipocytes and macrophages[15]. Thus, studies utilizing an inducible β-AR blocking strategy in a cell-specific manner (e.g., adipocytes versus macrophages) may provide important insight into how β-adrenergic signaling regulates joint inflammation under injury conditions. These findings may also be relevant to understanding the effect of exercise on OA joints.

A notable feature of our study was the identification of exercise-induced changes in synovial fluid metabolites using authenticated library standards. We previously reported on the effect of 1-night and 26-weeks of voluntary wheel running on murine synovial fluid metabolites using untargeted analyses[36,41]. The current study supports our previous findings for 1-night of exercise, such as increased amino acid, peptide, phospholipid, and bile acid metabolites. Compared to our previous untargeted analyses that identified > 1,000 metabolite features, the current validated analysis identified substantially fewer confirmed metabolites, which prevented us from

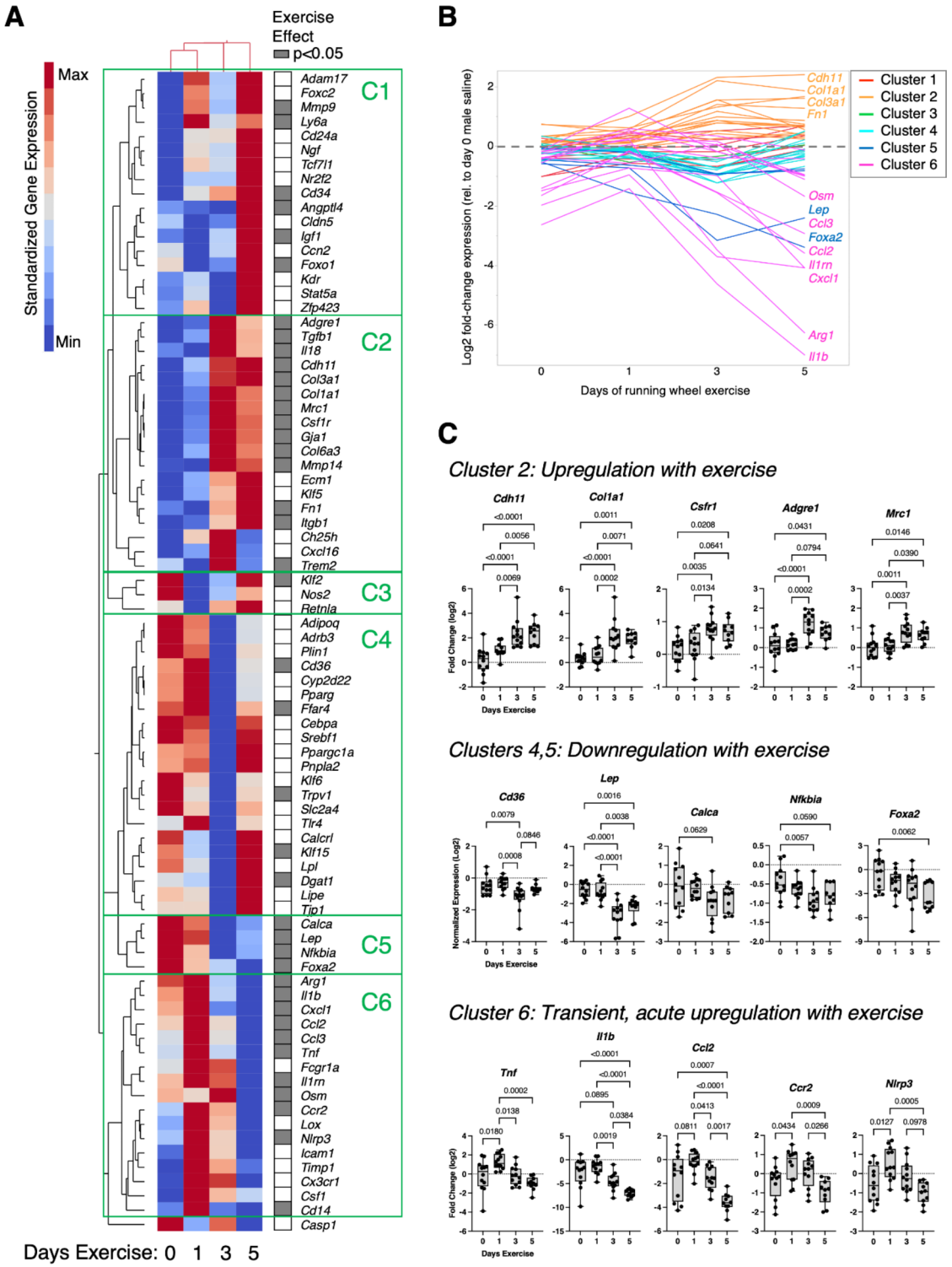

performing metabolic pathway enrichment analyses. Nevertheless, clear patterns were evident, such as an exercise-dependent increase in synovial fluid amino acids and peptides. Intriguingly, amino acids and peptides were similarly enriched in the synovial fluid of injured versus uninjured knees of humans and mice[27,55]. We also observed numerous similarities between exercise and injury in the subclasses of lipids that were enriched or diminished. For example, exercise and injury enriched sphingolipids, bile acids, medium straight chain fatty acids, and dicarboxylic acids, while diacylglycerols and hydroxy fatty acids were diminished[27]. Although the biological basis for this similarity between exercise and injury is not known, both conditions induce variable degrees of joint inflammation and IFP fibrosis, and inflammation has previously been associated with changes in serum lipid subclasses[56].

Synovial fluid is a key nutrient source for joint tissues, especially avascular tissues such as articular cartilage and the inner meniscus[57]. Therefore, it is important to consider the extent to which circulating blood metabolites

◀**Fig. 6**. Effect of short-term wheel running exercise on differential expression of targeted synovium-IFP genes. Gene expression was quantified by qRT-PCR using a Fluidigm 96.96 Dynamic Array IFC that included custom target genes related to inflammation, fibrosis, and adipose tissue homeostasis. Expression data were normalized to male, day-0, saline sample values and log2 transformed. Data were analyzed using a Mixed Model analysis, with exercise duration, treatment, and sex as "Fixed Effects" (including interaction terms). (**A**) 2-way hierarchical clustering analysis was used to identify patterns in gene expression across experimental groups. Heatmap color legend signifies standardized gene expression values calculated by subtracting the mean of log2-transformed values and dividing by the standard deviation. Columns represent mean values per experimental group, and rows show the targeted genes. Note that 0- and 1-day exercise conditions clustered together in the first and second columns. Filled cells in right-hand column indicate genes significantly altered by exercise (Mixed Model analysis; $p < 0.05$). Note, significant sex differences were only observed for 9 genes (*Cd34*, *Angptl4*, *Cldn5*, *Igf1*, *Foxo1*, *Ch25h*, *Cyp2d22*, *Klf6*, *Casp1*), and treatment effects were only observed for 4 genes (*Mmp9*, *Nfkbia*, *Icam1*, *Cx3cr1*) (Supplemental Table 6). (**B**) Line graphs of gene expression fold-change (log2) expressed by days of exercise and grouped by heatmap cluster (C1 – C6). (**C**) Boxplots of select genes within specific clusters show the 25th to 75th percentiles; horizontal line indicates the median, and whiskers denote maximum and minimum values ($n = 10–12$ per timepoint). Post-hoc paired comparisons evaluated by Tukey's multiple comparisons test ($p \leq 0.10$ shown).

contribute to the metabolic composition of synovial fluid. We previously reported that, in mice, synovial fluid and serum metabolites are largely distinct based on differences observed before and after a non-invasive compression knee injury[58]. A previous study in humans also found that less than 5% of metabolites were significantly correlated between synovial fluid and blood plasma[59]. Thus, synovial fluid likely represents a discrete metabolic niche. Nevertheless, increased blood flow during exercise could facilitate metabolic transport into the synovial fluid. We noted both similarities and differences in synovial fluid compared to endurance exercise-induced changes in serum metabolites[53,60,61]. In serum, one of the most upregulated metabolites following endurance exercise is the ketone 3-hydroxybutyrate (BHBA)[61]. BHBA is also upregulated in synovial fluid in the 1-day exercise group. Intriguingly, though, BHBA is not upregulated in synovial fluid after 3- and 5-days of exercise, suggesting a rapid adaptive response to repeated exercise. In serum, endurance exercise also upregulates central energy metabolites (e.g., lactate, α-ketoglutarate, succinate) and dicarboxylic fatty acids, and it reduces phospholipids and xenobiotics[61]. Dicarboxylic fatty acids are also elevated in synovial fluid after exercise, although other exercise effects are distinct, particularly changes in lipid subclasses, as previously discussed. Another notable difference is a robust increase in amino acids and peptides in synovial fluid, which are typically reduced in serum after endurance exercise[61]. Future longitudinal studies that directly compare synovial fluid and serum metabolites in the same exercising subjects are needed to confirm these literature-based comparisons.

There are limitations of this study that should be considered. The initial set of experiments involving 0-, 3-, and 14-day exercise timepoints only included male animals. Therefore, even though few sex differences were observed in experiments spanning 0- to 5-days of exercise, it is possible that more differences could emerge with longer exercise exposure. An additional limitation is the inability to clearly discriminate between myeloid cell populations in the flow cytometry experiments (e.g., neutrophils, infiltrating versus resident monocytes and macrophages). Methods that enable deep phenotyping, such as single-cell RNA sequencing or high-dimensional spectral flow cytometry, would provide valuable information to identify cell population changes in synovium-IFP tissue with exercise. Moreover, it should be recognized that OA changes the cellular populations, signaling networks, and structural property of joint tissues, including the synovium and IFP[62]. Therefore, while we have discussed the current results alongside studies evaluating the effect of exercise on OA joints, caution is warranted about extrapolating the current findings to OA patients. An important future study would be to evaluate the longitudinal trajectory of synovium-IFP inflammation after the initiation of exercise in joints with OA. Furthermore, it would be important to evaluate how exercise could also mitigate OA pain pathways by modifying inflammation outside of the joint, such as in the dorsal root ganglia.

Conclusions

Our study provides a time-resolved, integrated analysis of the effect of exercise on structural, inflammatory, and metabolic changes in synovium-IFP tissue. We demonstrate that initiating daily exercise using voluntary wheel running induces transient inflammation in synovium-IFP tissue. During the acute inflammatory period, exercise also causes IFP fibrosis, adipocyte atrophy, and altered synovial fluid metabolites, as previously observed for post-traumatic OA. Yet by 14 days of exercise, homeostasis is restored, and synovium-IFP structural and inflammatory outcomes return to pre-exercise levels. The translational impact of this work is the discovery that exercise provides a physiologically relevant model to study the induction and resolution of synovial joint inflammation. Exercise-based therapy is a core component of current clinical guidelines for treating knee OA, although the mechanisms by which exercise improves patient outcomes are not well understood. Thus, identifying the cellular, molecular, and metabolic transducers of exercise on joint tissues may better inform OA rehabilitation and treatment strategies.

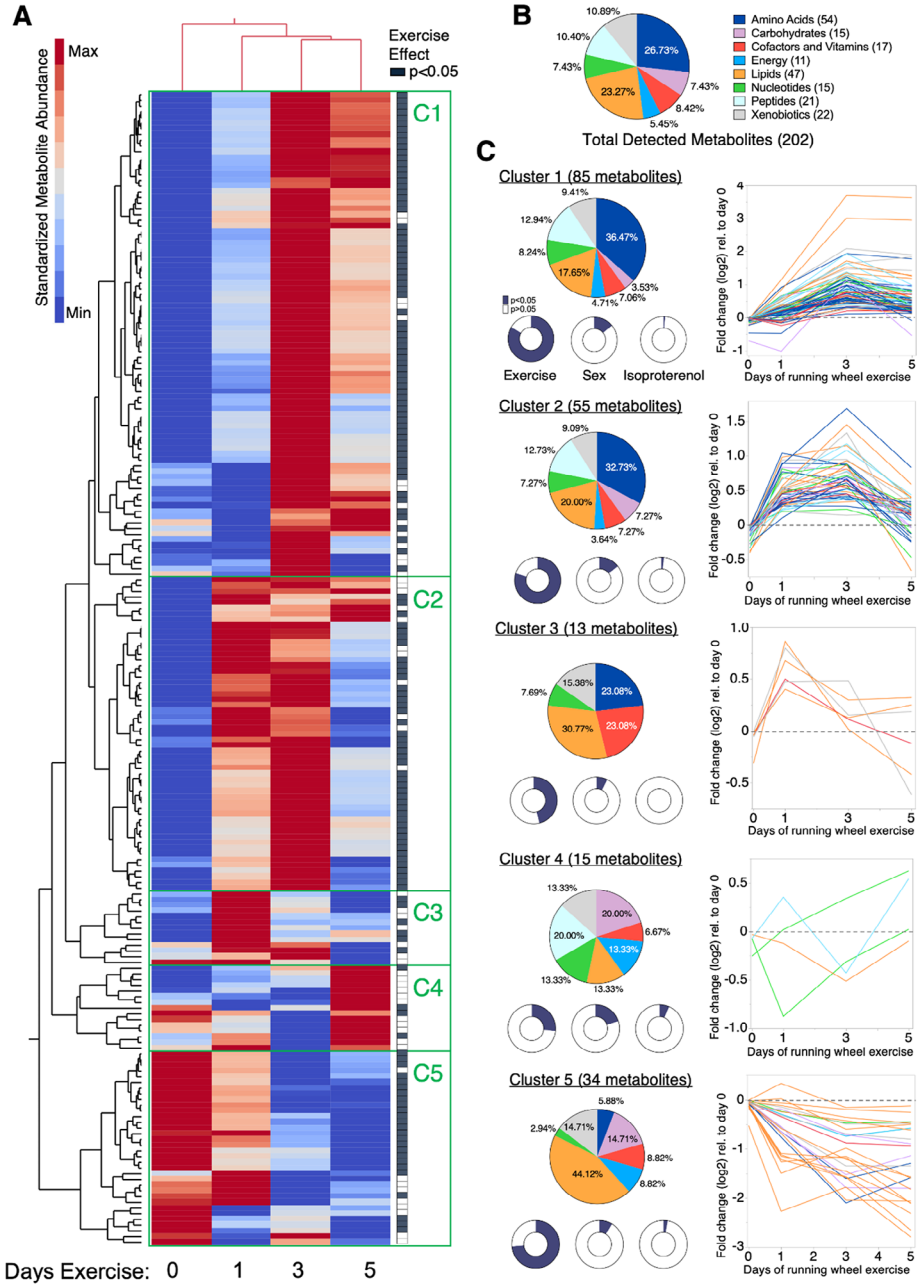

Fig. 7. Effect of short-term wheel running exercise on synovial fluid metabolites. Synovial fluid was collected from knees of male and female mice following 0, 1, 3, or 5 days of voluntary wheel running exercise and intra-articular injections, as described in Fig. 6. Samples were analyzed by Metabolon's Global Metabolomic Profiling Analysis, which identified 202 biochemicals confirmed by authenticated library standards. Peak area data were normalized to extracted volume and then median scaled. (**A**) 2-way hierarchical clustering analysis was used to identify patterns in synovial fluid metabolite abundance across experimental groups. Heatmap color legend signifies standardized metabolite values calculated by subtracting the mean and dividing by the standard deviation. Columns represent mean values per experimental group, and rows represent individual metabolites. Note that 3- and 5-day exercise conditions clustered together in the third and fourth columns. Filled cells in right-hand column indicate metabolites significantly altered by exercise (Generalized Linear Model including exercise, sex, and treatment effects). Green rectangles designate clusters (C1 – C5) with distinct changes in metabolite abundance versus days of exercise. (**B**) Pie chart of relative percent of all detected metabolites categorized by Metabolon's Metabolic Super Pathway assignment. Numbers in parentheses indicate absolute number of metabolites detected per category. (**C**) Pie charts of cluster-specific metabolite composition based on Metabolic Super Pathway assignments. Donut charts indicate the relative proportion of metabolites within a given cluster that were significantly altered by exercise, biological sex, or treatment ($p < 0.05$). Line graphs of metabolites significantly altered by exercise, expressed as abundance fold-change relative to day 0 values (log2) and color coded according to Metabolic Super Pathway (Supplemental Table 7).

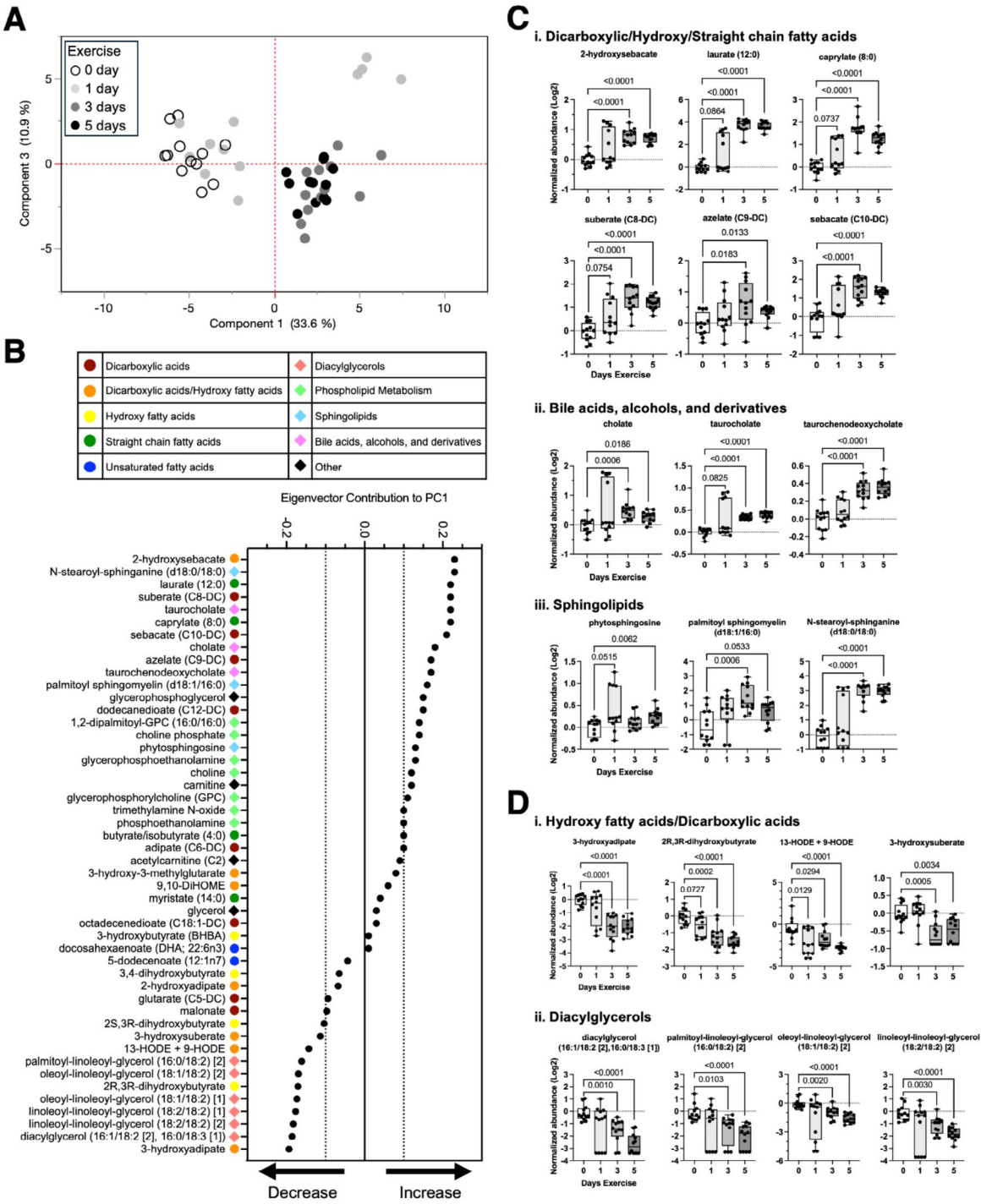

Fig. 8. Effect of short-term wheel running exercise on synovial fluid lipids. (**A**) Principal component (PC) analysis based on area-under-the-curve relative quantification of 47 lipids identified in the synovial fluid from a Global Metabolic Profiling Analysis (Metabolon). Symbols represent samples from knees of male and female mice treated with either saline or isoproterenol following 0, 1, 3, or 5 days of voluntary wheel running exercise. For simplicity, symbols only distinguish exercise duration, although a graph that also labels sex and treatment is available in Supplemental Fig. 3. (**B**) Variance along PC1 primarily corresponded to exercise duration. Therefore, eigenvector contributions of lipid species to PC1 were plotted in descending value to identify candidate lipid species most sensitive to exercise. Colors and symbols in the key identify the super pathway assignment for each lipid, according to Metabolon. (**C**) Boxplots of lipids that were upregulated or (**D**) downregulated with increasing exercise duration show the 25th to 75th percentiles, with horizontal line indicating the median, and whiskers denoting maximum and minimum values ($n = 10–12$ per timepoint). Data analyzed by Brown-Forsythe ANOVA with Dunnett's T3 multiple comparisons post-hoc test ($p \leq 0.10$ shown).

Data availability

The synovial fluid metabolomic data file is available in supplemental material. All other datasets used for the present study are available from the corresponding author upon reasonable request.

Received: 25 September 2024; Accepted: 13 January 2025
Published online: 18 January 2025

References

1. Decker, R. S. et al. Cell origin, volume and arrangement are drivers of articular cartilage formation, morphogenesis and response to injury in mouse limbs. *Dev. Biol.* **426**, 56–68 (2017).
2. Roelofs, A. J. et al. Joint morphogenetic cells in the adult mammalian synovium. *Nat. Commun.* **8** (15040). https://doi.org/10.1038/ncomms15040 (2017).
3. Loeser, R. F., Goldring, S. R., Scanzello, C. R., Goldring, M. B. & Osteoarthritis A disease of the joint as an organ. *Arthritis Rheum.* **64**, 1697–1707 (2012).
4. Lories, R. J. & Luyten, F. P. The bone-cartilage unit in osteoarthritis. *Nat. Rev. Rheumatol.* **7**, 43–49 (2011).
5. Englund, M. et al. Meniscal tear in knees without surgery and the development of radiographic osteoarthritis among middle-aged and elderly persons: the multicenter osteoarthritis study. *Arthritis Rheum.* **60**, 831–839 (2009).
6. Emmanuel, K. et al. Quantitative measures of meniscus extrusion predict incident radiographic knee osteoarthritis – data from the Osteoarthritis Initiative. *Osteoarthr. Cartil.* **24**, 262–269 (2016).
7. Pap, T., Dankbar, B., Wehmeyer, C., Korb-Pap, A. & Sherwood, J. Synovial fibroblasts and articular tissue remodelling: role and mechanisms. *Semin Cell. Dev. Biol.* **101**, 140–145 (2020).
8. Knights, A. J. et al. Synovial fibroblasts assume distinct functional identities and secrete R-spondin 2 in osteoarthritis. *Ann. Rheum. Dis.* **82**, 272–282 (2022).
9. Clockaerts, S. et al. The infrapatellar fat pad should be considered as an active osteoarthritic joint tissue: a narrative review. *Osteoarthr. Cartil.* **18**, 876–882 (2010).
10. Ioan-Facsinay, A. & Kloppenburg, M. An emerging player in knee osteoarthritis: the infrapatellar fat pad. *Arthritis Res. Therapy*. **15**, 225 (2013).
11. Eymard, F. & Chevalier, X. Inflammation of the infrapatellar fat pad. *Joint Bone Spine*. **83**, 389–393 (2016).
12. Han, W. et al. Association between Quantitatively Measured Infrapatellar Fat Pad High Signal-Intensity Alteration and magnetic resonance imaging–assessed progression of knee osteoarthritis. *Arthrit Care Res.* **71**, 638–646 (2019).
13. Zhou, S. et al. Source and hub of inflammation: the infrapatellar fat pad and its interactions with articular tissues during knee osteoarthritis. *J. Orthop. Res.* **40**, 1492–1504 (2022).
14. Ioan-Facsinay, A., Kloppenburg, M. & Osteoarthritis Inflammation and fibrosis in adipose tissue of osteoarthritic joints. *Nat. Rev. Rheumatol.* **13**, 325–326 (2017).
15. Li, J. et al. Synovium and infrapatellar fat pad share common mesenchymal progenitors and undergo coordinated changes in osteoarthritis. *J. Bone Min. Res.* **39**, 161–176 (2024).
16. Griffin, T. M. & Lories, R. J. Cracking the code on the innate immune program in OA. *Osteoarthr. Cartil.* **28**, 529–531 (2020).
17. Davis, A. M., Davis, K. D., Skou, S. T. & Roos, E. M. Why is Exercise Effective in reducing Pain in people with Osteoarthritis? *Curr. Treat. Options Rheumatol.* **6**, 146–159 (2020).
18. Holden, M. A. et al. Recommendations for the delivery of therapeutic exercise for people with knee and/or hip osteoarthritis. An international consensus study from the OARSI Rehabilitation Discussion Group. *Osteoarthr. Cartil.* **31**, 386–396 (2023).
19. Ambrosi, D. et al. Perspectives on biological growth and remodeling. *J. Mech. Phys. Solids*. **59**, 863–883 (2011).
20. Verbruggen, S. W. et al. Stresses and strains on the human fetal skeleton during development. *J. R Soc. Interface*. **15**, 20170593 (2018).
21. Issa, R., Boeving, M., Kinter, M. & Griffin, T. M. Effect of biomechanical stress on endogenous antioxidant networks in bovine articular cartilage. *J. Orthop. Res.* **36**, 760–769 (2018).
22. Dossumbekova, A. et al. Biomechanical signals inhibit IKK activity to attenuate NF-kappaB transcription activity in inflamed chondrocytes. *Arthritis Rheum.* **56**, 3284–3296 (2007).
23. Nam, J. et al. Transcriptome-wide gene regulation by gentle treadmill walking during the progression of monoiodoacetate-induced arthritis. *Arthritis Rheum.* **63**, 1613–1625 (2011).
24. Pendyala, M. et al. Endogenous production of hyaluronan, PRG4, and cytokines is sensitive to cyclic loading in synoviocytes. *Plos One*. **17**, e0267921 (2022).
25. Shoham, N. & Gefen, A. Mechanotransduction in adipocytes. *J. Biomech.* **45**, 1–8 (2012).
26. Wang, M. et al. Knee fibrosis is associated with the development of osteoarthritis in a murine model of tibial compression. *J. Orthop. Res.* **39**, 1030–1040 (2021).
27. Komaravolu, R. K. et al. Sex-specific effects of injury and beta-adrenergic activation on metabolic and inflammatory mediators in a murine model of post-traumatic osteoarthritis. *Osteoarthr. Cartil.* **32**, 1097–1112 (2024).
28. Thompson, D., Karpe, F., Lafontan, M. & Frayn, K. Physical activity and Exercise in the regulation of human adipose tissue physiology. *Physiol. Rev.* **92**, 157–191 (2012).
29. Chow, L. S. et al. Exerkines in health, resilience and disease. *Nat. Rev. Endocrinol.* **18**, 273–289 (2022).
30. Winn, N. C., Cottam, M. A., Wasserman, D. H. & Hasty, A. H. Exercise and Adipose tissue immunity: outrunning inflammation. *Obesity* **29**, 790–801 (2021).
31. Lehnig, A. C., Stanford, K. I., Suarez, R. K. & Hoppeler, H. H. Exercise-induced adaptations to white and brown adipose tissue. *J. Exp. Biol.* **221**, jeb161570 (2018).
32. Donovan, E. L., Lopes, E. B. P., Batushansky, A., Kinter, M. & Griffin, T. M. Independent effects of dietary fat and sucrose content on chondrocyte metabolism and osteoarthritis pathology in mice. *Dis. Models Mech.* **11**, dmm034827 (2018).
33. Galarraga, M. et al. Adiposoft: automated software for the analysis of white adipose tissue cellularity in histological sections. *J. Lipid Res.* **53**, 2791–2796 (2012).
34. Barboza, E. et al. Profibrotic Infrapatellar Fat Pad Remodeling without M1 Macrophage polarization precedes knee osteoarthritis in mice with Diet-Induced obesity. *Arthritis Rheum.* **69**, 1221–1232 (2017).
35. Que, X. et al. Oxidized phospholipids are Proinflammatory and proatherogenic in Hypercholesterolemic mice. *Nature* **558**, 301–306 (2018).
36. Hahn, A. K. et al. Effects of long-term exercise and a high-fat diet on synovial fluid metabolomics and joint structural phenotypes in mice: an integrated network analysis. *Osteoarthr. Cartil.* **29**, 1549–1563 (2021).
37. Zhivaki, D. & Kagan, J. C. Innate immune detection of lipid oxidation as a threat assessment strategy. *Nat. Rev. Immunol.* **22**, 322–330 (2022).
38. Irintchev, A. & Wernig, A. Muscle damage and repair in voluntarily running mice: strain and muscle differences. *Cell. Tissue Res.* **249**, 509–521 (1987).
39. Collins, S. β-Adrenergic receptors and adipose tissue metabolism: evolution of an Old Story. *Annu. Rev. Physiol.* **84**, 1–16 (2022).

40. Lamkin, D. M. et al. β-Adrenergic-stimulated macrophages: comprehensive localization in the M1-M2 spectrum. *Brain Behav. Immun.* **57**, 338–346 (2016).
41. Hahn, A. K. et al. In vivo mechanotransduction: Effect of acute exercise on the metabolomic profiles of mouse synovial fluid. *Osteoarthr. Cartil. Open.* **4**, 100228 (2022).
42. Helmark, I. C. et al. Exercise increases interleukin-10 levels both intraarticularly and peri-synovially in patients with knee osteoarthritis: a randomized controlled trial. *Arthritis Res. Therapy*. **12**, 1–11 (2010).
43. Hyldahl, R. D. et al. Running decreases knee intra-articular cytokine and cartilage oligomeric matrix concentrations: a pilot study. *Eur. J. Appl. Physiol.* **116**, 2305–2314 (2016).
44. Jayabalan, P., Gustafson, J., Sowa, G. A., Piva, S. R. & Farrokhi, S. A. Stimulus-response Framework to investigate the influence of continuous versus interval walking Exercise on Select serum biomarkers in knee osteoarthritis. *Am. J. Phys. Med. Rehabilitation*. **98**, 287–291 (2019).
45. Bricca, A. et al. Impact of Exercise Therapy on molecular biomarkers related to cartilage and inflammation in individuals at risk of, or with established, knee osteoarthritis: a systematic review and Meta-analysis of Randomized controlled trials. *Arthritis Care Res.* **71**, 1504–1515 (2019).
46. Oka, Y. et al. Mild treadmill exercise inhibits cartilage degeneration via macrophages in an osteoarthritis mouse model. *Osteoarthr. Cartil. Open.* **5**, 100359 (2023).
47. Bandak, E. et al. The effect of exercise therapy on inflammatory activity assessed by MRI in knee osteoarthritis: secondary outcomes from a randomized controlled trial. *Knee* **28**, 256–265 (2021).
48. Bannuru, R. R. et al. OARSI guidelines for the non-surgical management of knee, hip, and polyarticular osteoarthritis. *Osteoarthr. Cartil.* **27**, 1578–1589 (2019).
49. Kolasinski, S. L. et al. 2019 American College of Rheumatology/Arthritis Foundation Guideline for the Management of Osteoarthritis of the Hand, hip, and Knee. *Arthrit Care Res.* **72**, 149–162 (2020).
50. Henriksen, M., Runhaar, J., Turkiewicz, A. & Englund, M. Exercise for knee osteoarthritis pain: Association or causation? *Osteoarthr. Cartil.* **32**, 643–648 (2024).
51. Hawley, J. A., Joyner, M. J. & Green, D. J. Mimicking exercise: what matters most and where to next? *J. Physiol.* **599**, 791–802 (2021).
52. MoTrPAC Study Group Primary authors. Temporal dynamics of the multi-omic response to endurance exercise training. *Nature* **629**, 174–183 (2024).
53. Contrepois, K. et al. Molecular choreography of Acute Exercise. *Cell* **181**, 1112–1130 (2020).
54. Methenitis, S., Stergiou, I., Antonopoulou, S. & Nomikos, T. Can Exercise-Induced Muscle Damage Be a Good Model for the Investigation of the Anti-Inflammatory Properties of Diet in Humans? *Biomedicines*. 9, 36 (2021).
55. Welhaven, H. D. et al. Metabolic phenotypes reflect patient sex and Injury Status: a cross-sectional analysis of human synovial fluid. *Osteoarthr. Cartil.* **32**, 1074–1083 (2024).
56. Hornburg, D. et al. Dynamic lipidome alterations associated with human health, disease and ageing. *Nat. Metab.* **5**, 1578–1594 (2023).
57. Wallace, C. W. et al. Correlations between metabolites in the synovial fluid and serum: a mouse injury study. *J. Orthop. Res.* **40**, 2792–2802 (2022).
58. Zhang, W. et al. Relationship between blood plasma and synovial fluid metabolite concentrations in patients with osteoarthritis. *J. Rheumatol.* **42**, 859–865 (2015).
59. Lewis, G. D. et al. Metabolic signatures of Exercise in Human plasma. *Sci. Transl Med.* **2**, 33ra37–33ra37 (2010).
60. Morville, T., Sahl, R. E., Moritz, T., Helge, J. W. & Clemmensen, C. Plasma metabolome profiling of Resistance Exercise and endurance Exercise in humans. *Cell. Rep.* **33**, 108554 (2020).
61. Schranner, D., Kastenmüller, G., Schönfelder, M., Römisch-Margl, W. & Wackerhage, H. Metabolite Concentration changes in humans after a Bout of Exercise: a systematic review of Exercise Metabolomics studies. *Sports Med. - Open.* **6**, 1–17 (2020).
62. Tang, S. et al. Single-cell atlas of human infrapatellar fat pad and synovium implicates APOE signaling in osteoarthritis pathology. *Sci. Transl Med.* **16**, eadf4590 (2024).

Acknowledgements

The authors gratefully acknowledge assistance from the OMRF Imaging Core Facility and OMRF Flow Cytometry and Cell Sorting Core Facility for sample processing. We also acknowledge Tatsiana Akraiko and Mark Band of the Carver Biotechnology Center, Functional Genomics Lab, University of Illinois for Fluidigm qPCR processing.

Author contributions

Concept and design: TMG, EBPL, SK, RKJ; acquisition, analysis, and interpretation of data: TMG, RKK, EBPL, PMD, TC, TK, SK, MA, PH, MBH, HW, PB, and RKJ; TMG drafted the manuscript and RKK, EBPL, PMD, TC, TK, SK, MA, PH, MBH, HW, PB, and RKJ critically reviewed and revised it; final approval of article provided by TMG, RKK, EBPL, PMD, TC, TK, SK, MA, PH, MBH, HW, PB, and RKJ. Note, EBPL and TC oversaw animal group and treatment allocation and blinded identification assignments.

Funding

Supported by the National Institute of Arthritis and Musculoskeletal and Skin Diseases (R03AR066828, R01AR073964, and R01AR081489), the Department of Veterans Affairs (I01BX004666, I01BX004882), and the Oklahoma Medical Research Foundation. The content is solely the responsibility of the authors and does not necessarily represent the official views of the National Institutes of Health, the Department of Veterans Affairs, or the Oklahoma Medical Research Foundation.

Declarations

Competing interests

TM Griffin: Patent application pending entitled, "COMPOSITIONS AND METHODS FOR TREATING OSTEOARTHRITIS USING A CD14 INHIBITOR" (#18/411,242); consulting – Novo Nordisk. P Brahmachary: Owns stock in OpenBioWorks. RK June: Owns stock in Beartooth Biotech and OpenBioWorks. No other authors report competing interests.

Ethics approval

All animals were housed and handled under veterinary oversight in the animal facility at the Oklahoma Medical Research Foundation (OMRF). All procedures were conducted following protocols approved by the AAALAC-accredited Institutional Animal Care and Use Committees at OMRF (protocol 12–47, 14–19, 17–24, 19–49, and 22–60) and Oklahoma City VA (protocol 1907-001).

Additional information

Supplementary Information The online version contains supplementary material available at https://doi.org/10.1038/s41598-025-86726-0.

Correspondence and requests for materials should be addressed to T.M.G.

Reprints and permissions information is available at www.nature.com/reprints.

Publisher's note Springer Nature remains neutral with regard to jurisdictional claims in published maps and institutional affiliations.

Open Access This article is licensed under a Creative Commons Attribution-NonCommercial-NoDerivatives 4.0 International License, which permits any non-commercial use, sharing, distribution and reproduction in any medium or format, as long as you give appropriate credit to the original author(s) and the source, provide a link to the Creative Commons licence, and indicate if you modified the licensed material. You do not have permission under this licence to share adapted material derived from this article or parts of it. The images or other third party material in this article are included in the article's Creative Commons licence, unless indicated otherwise in a credit line to the material. If material is not included in the article's Creative Commons licence and your intended use is not permitted by statutory regulation or exceeds the permitted use, you will need to obtain permission directly from the copyright holder. To view a copy of this licence, visit http://creativecommons.org/licenses/by-nc-nd/4.0/.

© The Author(s) 2025